

PROPAGATION CHARACTERISTICS OF ELECTROMAGNETIC WAVES IN THIN FILMS WITH NONLINEAR MATERIAL

J. R. Souza

Centro de Estudos em Telecomunicações - CETUC  
Pontifícia Universidade Católica do Rio de Janeiro - PUC/Rio  
Rua Marquês de São Vicente, 225  
22453 Rio de Janeiro - RJ, Brasil

ABSTRACT:

The propagation characteristics of electromagnetic waves in thin films with nonlinear material are investigated numerically using variational methods and finite difference techniques. Both TE and TM polarizations are considered. It is observed that hysteresis and bistability can occur. It is also observed that part of the higher order solutions may be unstable and may follow a route to chaos through period doubling as the guided wave power increases.

1. INTRODUCTION

Dielectric waveguides, or thin films, with nonlinear material have attracted considerable interest in recent years due to their unique, fascinating features, and potential application to devices for an all-optical signal processor, as well as for optical computers [1].

The knowledge of the propagation characteristics of electromagnetic waves in such structures is necessary not only to determine the feasibility of the suggested devices, but also to further the understanding of the physical phenomena associated with nonlinear guided waves systems. Of particular interest is the study of the stability characteristics of waves guided by such structures, as this will determine the limit of their usability.

Stability analyses of TE nonlinear guided waves can be found in the literature, e.g. [2]-[8]. References [2]-[7] present the stability analysis of TE waves guided by a thin film bounded by semi-infinite nonlinear media, while reference [8] deals with TE waves guided by a nonlinear film bounded by semi-infinite linear media. With the exception of reference [2], where a stability theory was developed for the fundamental TE mode, the other conclusions and results reported in the literature [3]-[8] were obtained by launching a specific electric field profile into the waveguide and numerically simulating its propagation down the waveguide. Reference [3]-[7] have in common the numerical method employed in the simulated propagation: the Beam

Propagation Method (BPM). In [8], the wave propagation is simulated by means of the finite element method. So far, no stability analysis has been carried out for nonlinear TM guided waves.

This paper presents a new formulation for the stability analysis of nonlinear guided waves. It was developed [9]-[11] in order to investigate to what extent the results and conclusions reported in the literature depend on the numerical techniques used. It is applied to both TE and TM nonlinear guided waves.

2. FORMULATION

Figure 1 shows the waveguides considered, where the three layers can be of nonlinear material.

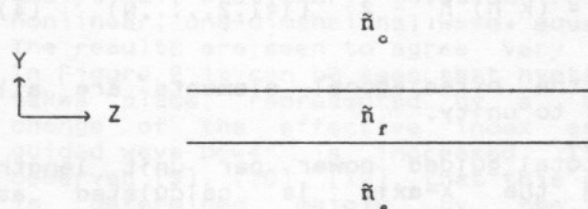


Figure 1: Nonlinear waveguide.

For TE polarization, the nonlinear refractive index is written as [13]:

$$\tilde{n}_j^2 = n_j^2 + a_j f(S) \quad , \quad j = s, f, c \quad (1)$$

where  $n_j$  represents the low power refractive index, which may be a function of  $y$ ,  $a_j$  represents the nonlinear coefficient of medium  $j$  ( $j=s, f, c$ ) and  $f(S)$ , a function of the signal intensity  $S$ . For Kerr-type nonlinearity,  $f(S) = |E|^2$ , where  $E$  denotes the electric field. In this case, each coefficient  $a_j$  is then written as  $n_j n_{j,c} \epsilon_0$ ,  $n_j$  being the nonlinear coefficient,  $\epsilon_0$  the free space permittivity, and  $c$  the velocity of light in vacuum.

Assuming that the waveguide is composed of lossless media, and that  $\partial/\partial X = 0$ , a variational expression for the propagation

constant  $\beta$  for TE waves is written as [9]-[11]:

$$\beta^2 = \left[ \int_{-\infty}^{\infty} \left[ k_0^2 \tilde{n}^2 E_x^2 - \left( \frac{dE_x}{dy} \right)^2 \right] dy \right] \cdot \left[ \int_{-\infty}^{\infty} E_x^2 dy \right]^{-1} \quad (2)$$

where  $E$  is the X-component of the electric field,  $k_0$  is the free space wavenumber, and the  $\circ$  factor  $\exp[j(\omega t - \beta z)]$  is implicit.

Next, the Y-axis is discretized, finite differences are used to evaluate the derivative in the expression for  $\beta^2$ , and the integrals in (2) are approximated in terms of the discretized field.

The stationary property of  $\beta^2$  is then used through the differentiation of (2) with respect to each of the variables  $E$ , where  $E_i$  is the value of  $E$  at  $y = y_i$ ,  $i = 1, 2, \dots, N$ ,  $E_0$  and  $E_{N+1}$  being set to zero. The following standard eigenvalue problem is arrived at [9]-[11]:

$$[A] \cdot \{E_x\} = (\beta h)^2 \cdot \{E_x\} \quad (3)$$

where  $h$  is the distance between successive points along the Y-axis,  $[A]$  is a real, symmetrical and tridiagonal matrix, whose diagonal elements are given by [9]-[11]:

$$A_{ii} = (k_0 h)^2 \tilde{n}_i^2 - 2 \quad (i=1, 2, \dots, N) \quad (4)$$

and the off-diagonal elements are all equal to unity.

The total guided power per unit length along the X-axis is calculated as [9]-[11]:

$$P = \frac{\beta}{2k_0 Z_0} \int_{-\infty}^{\infty} E_x^2 dy \quad (5)$$

where  $Z_0$  represents the intrinsic impedance of vacuum.

Considering Kerr-type nonlinearity, for TM polarization the nonlinear permittivity is written as [10],[14]:

$$\begin{aligned} \epsilon_{xj} &= n_j^2 \\ \epsilon_{yj} &= \tilde{n}_{yj}^2 = n_j^2 + \epsilon_0 c n_j^2 n_{2j} \cdot (|E_y|^2 + \gamma |E_z|^2) \\ \epsilon_{zj} &= \tilde{n}_{zj}^2 = n_j^2 + \epsilon_0 c n_j^2 n_{2j} \cdot (\gamma |E_y|^2 + |E_z|^2) \end{aligned} \quad (6)$$

where  $\epsilon_j$ ,  $c$ , and  $\epsilon_0$  are diagonal elements of the permittivity tensor,  $n_j$  represents the low power refractive index of medium  $j$ .  $E_y$  and  $E_z$  are, respectively, the Y- and Z-components of the electric

field. The constant  $\gamma$  takes on different values, depending on the nonlinearity mechanism [14], and will here be fixed as 1.

As in the case of TE polarization, a variational expression is first developed for the propagation constant  $\beta$  [9],[11]:

$$\beta^2 = \frac{\int_{-\infty}^{\infty} \frac{1}{\epsilon_z} (dH_x/dy)^2 dy - k_0^2 \int_{-\infty}^{\infty} H_x^2 dy}{\int_{-\infty}^{\infty} \frac{1}{\epsilon_y} H_x^2 dy} \quad (7)$$

Following the same steps as in the case of TE polarization, the standard eigenvalue problem is obtained [9],[11]:

$$[B] \cdot \{H_x\} = (\beta h)^2 \cdot \{H_x\} \quad (8)$$

where  $H_x$  is the X-component of the magnetic field,  $[B]$  is a real tridiagonal matrix, whose elements are given by [9],[11]:

$$\begin{aligned} B_{ii} &= \left( k_0^2 h^2 - \frac{1}{\epsilon_{zi-1}} - \frac{1}{\epsilon_{zi}} \right) \cdot \epsilon_{yi} \\ B_{i,i+1} &= \frac{\epsilon_{yi}}{\epsilon_{zi}} \\ B_{i-1,i} &= \frac{\epsilon_{yi}}{\epsilon_{zi-1}} \end{aligned} \quad (9)$$

The total guided power per unit length along the X-axis is calculated as:

$$P = \frac{1}{2} \cdot \frac{Z_0 \beta}{k_0} \cdot \int_{-\infty}^{\infty} \frac{1}{\epsilon_y} H_x^2 dy \quad (10)$$

The solution of the eigenvalue problems yields the propagation constant  $\beta$  and the electric field profile, in the case of TE waves, or the magnetic field profile, in the case of TM waves.

As in the presence of nonlinearity the refractive index distribution depends on the local field intensity, an iterative scheme is used in the solution of the eigenvalue problems (3) and (8). For each polarization, the eigenvalue problem is initially solved assuming negligible power

level. The resulting electric (or magnetic) field is then scaled to the required power level, and used to update the refractive index distribution due to the nonlinear contributions, and the eigenvalue problem is solved again. This iterative scheme continues until consistent solutions are obtained.

### 3. RESULTS

In all the results presented here, only Kerr-type nonlinearity was considered, in order to allow comparison with other results in the literature.

Figure 2 shows the variation of the fundamental mode TE effective refractive index  $\beta/k$  with the guided wave power for a structure composed of a linear film, whose thickness is  $1.25\mu\text{m}$  and refractive index is 1.57, bounded by identical, semi-infinite nonlinear substrate and cladding, with a low power refractive index of  $1.0 \times 10^{-9} \text{m}^2/\text{W}$ . The wavelength is  $0.515\mu\text{m}$ .

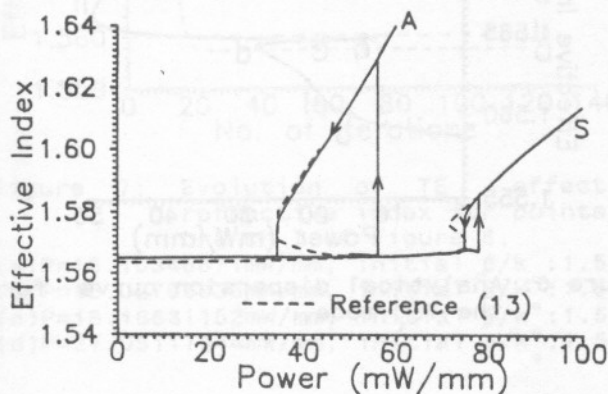


Figure 2: Variation of the TE effective refractive index with guided wave power.

This fundamental mode presents two solutions: one, with a symmetrical electric field distribution with respect to the X-axis, that evolves from the corresponding solution in a similar, linear waveguide. This solution is represented by curve S in Figure 2. For power levels above a certain value, a second solution appears, in which the electric field distribution is asymmetrical with respect to the X-axis, curve A in Figure 2. It was observed that, for power levels where the asymmetrical solution exists, the symmetrical solution is unstable, i.e. it is not maintained along the iterative scheme. This situation is illustrated in Figure 3, which shows the evolution of the solution with the iterative scheme. In this Figure it is clearly seen that the symmetrical solution

gives place to the asymmetrical solution, which is maintained indefinitely along the iterative scheme.

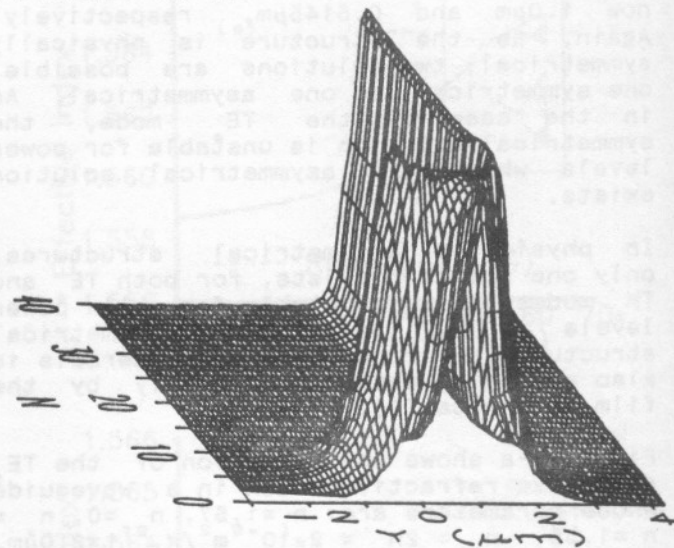


Figure 3: Evolution of the TE electric field profile with the iterative scheme, with  $P = 95 \text{mW/mm}$ .

Figure 2 also shows results as read from reference [13], which presents an analytical, stationary solution for the nonlinear, one-dimensional wave equation. The results are seen to agree very well. In Figure 2 it can be seen that hysteresis takes place, represented by a sudden change of the effective index as the guided wave power is increased. It was observed [9], [10], [12], that this effect is determined mainly by the film thickness, and that it can occur at low power levels. Such effect has potential application in fast optical switches or memory loops [1].

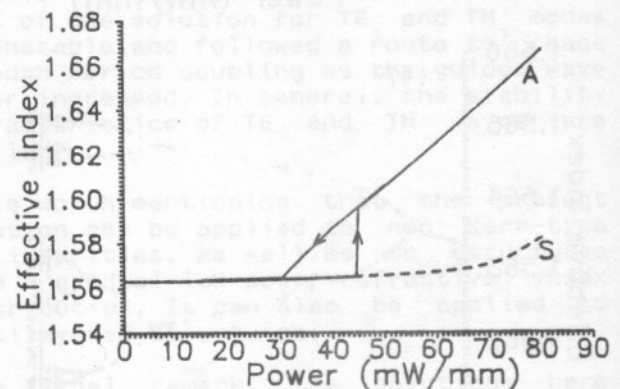


Figure 4: Variation of the TM effective refractive index with guided wave power.

Figure 4 shows, for the TM mode, the variation of the effective refractive index with guided wave power in a

structure with the same parameters as that of Figure 2, with the exception of the film thickness and wavelength, which are now  $1.0\mu\text{m}$  and  $0.5145\mu\text{m}$ , respectively. Again, as the structure is physically symmetrical, two solutions are possible, one symmetrical and one asymmetrical. As in the case of the TE mode, the symmetrical solution is unstable for power levels where the asymmetrical solution exists.

In physically asymmetrical structures, only one solution exists, for both TE and TM modes, which is stable for all power levels [9], [11]. In asymmetrical structures the occurrence of hysteresis is also possible, determined mainly by the film thickness [9], [10].

Figure 5-a shows the variation of the TE effective refractive index in a waveguide whose parameters are:  $n_1=1.57$ ,  $n_2=0$ ,  $n_3 = n_1=1.55$ ,  $n_4 = 2n_3 = 2 \times 10^{-9} \text{m}^2/\text{W}$ ,  $2r_1t=2.0\mu\text{m}$ , and the wavelength  $\lambda_0$  is  $0.515\mu\text{m}$ . The solid line represents solutions for which the iterative scheme converged to a single value of the effective index and a single profile for the electric field. The dotted lines represent solutions for which the iterative scheme did not converge to a

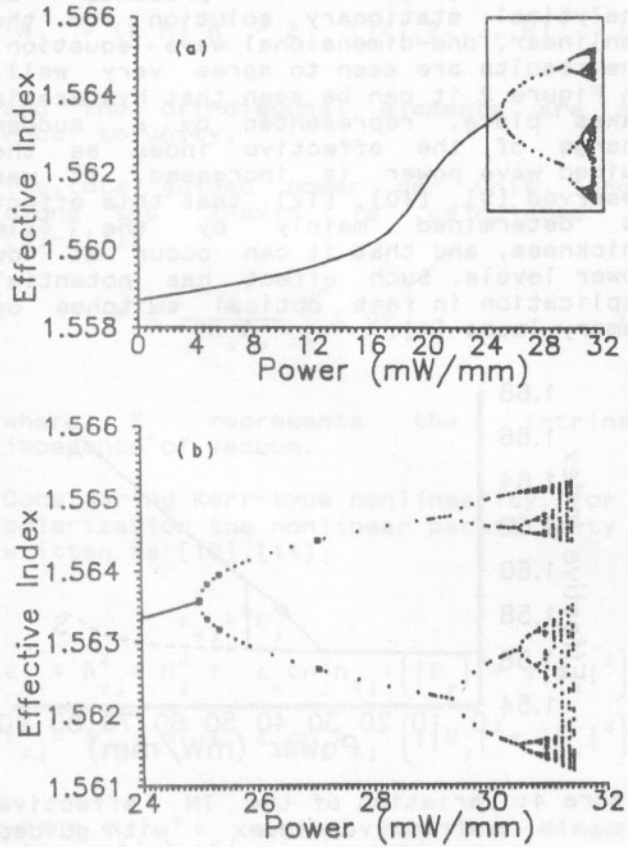


Figure 5: Bifurcation diagram for the variation of the TE effective refractive index with guided wave power.

single value of the effective index (and a electric field single profile), but resulted in multiple values, which are periodic with respect to the iterations. Initially, period two oscillations are observed, which give place to period four oscillations as the guided wave power increases, and then to period eight oscillations, and so on, until chaotic oscillations appear. The boxed part of Figure 5-a is enlarged in Figure 5-b, showing clearly the transition to chaos through period doubling.

The analytical stationary solution of reference [7] and [13] was used as comparison and mainly to help identifying stable and unstable solutions. Figure 6 shows two of the three branches of the analytical, stationary solution for the TE mode in the same waveguide as in Figures 5.

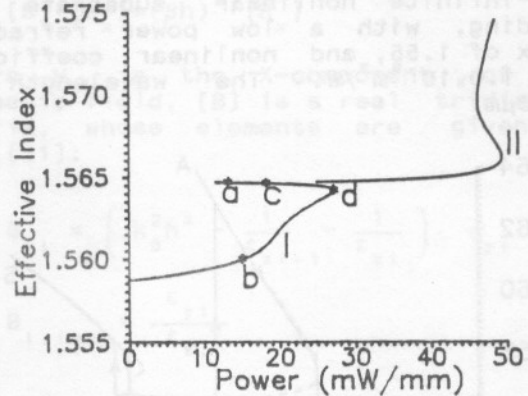


Figure 6: Analytical dispersion curve for the TE<sub>1</sub> mode.

The effective refractive index and electric field profile given by this analytical solution were used as input data for the eigenvalue problem and the iterative scheme. Identical results as in Figures 5 were obtained. It was observed that at low power levels, i.e. the initial part of branch I in Figure 6, the solution was maintained along the iterative scheme. For power where the two branches existed simultaneously, period two oscillations were observed. The oscillation period doubled along branch II as the guided wave power increased. The second part of branch I, after the peak, showed a different behavior: after a few iterations, the solution converged to values corresponding to points on the other side of the branch (before the peak). These results are summarized in Figure 7, which shows the evolution of the effective index with the iterative process, for certain power levels.

It is interesting to note that once the

oscillations start, points originally on either branch fit the same bifurcation diagram, as illustrated in Figure 5-b, where the squares correspond to points originally on branch I and the dots, to points originally on branch II. According to these results, the first part of branch I, up to the power level where branch II starts (solid line in Figures 5) is considered as stable. The second part of branch I, after the peak and not co-existing with branch II, is considered as unstable. All the rest of the solution is considered as unstable and may follow a route to chaos through period doubling as the guided wave power increases (dotted lines in Figures 5).

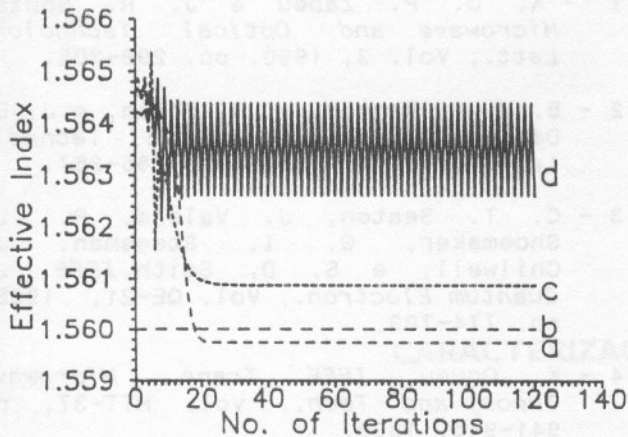


Figure 7: Evolution of TE effective refractive index for points on branch I of Figure 6.  
 (a)  $P=13.10346571\text{mW/mm}$ , initial  $\beta/k^\circ:1.56470$   
 (b)  $P=15.02796935\text{mW/mm}$ , initial  $\beta/k^\circ:1.560$   
 (c)  $P=18.18631152\text{mW/mm}$ , initial  $\beta/k^\circ:1.56465$   
 (d)  $P=27.05117944\text{mW/mm}$ , initial  $\beta/k^\circ:1.56422$

Figures 8 show a bifurcation diagram for the TM mode in a waveguide with the same parameters as in Figures 5 and 6, except for  $n_2 = n_1 = 1.0 \times 10^{-9} \text{ m}^2/\text{W}$  and the wavelength is  $0.5145 \mu\text{m}$ . Again it was observed that part of the solution was unstable, dotted lines, and followed a route to chaos through period doubling as the guided wave power increased. Figure 8-a also shows results as read from reference [14], which presents an analytical, stationary solution for nonlinear TM waves. A very good agreement is seen for the stable part of the solution. As the analytical solution of reference [14] is stationary, it is unable to predict the unstable part.

4. CONCLUSION

A numerical solution was developed and applied to the analysis of TE and TM waves in waveguides containing nonlinear

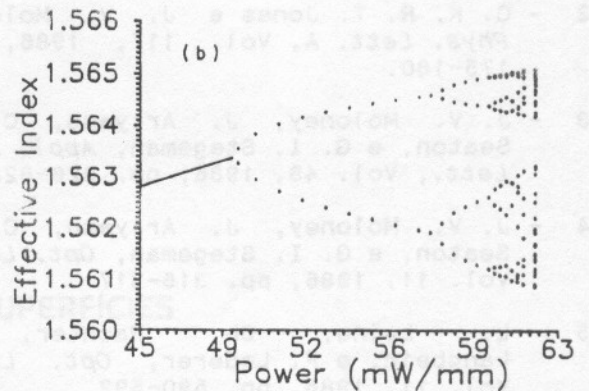
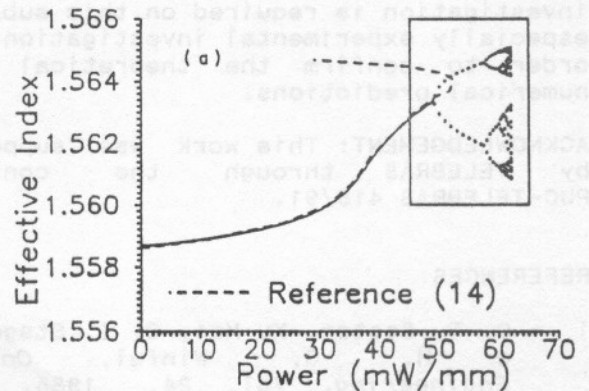


Figure 8: Bifurcation diagram for the variation of the TM effective refractive index with guided wave power.

material. For the fundamental modes TE and TM it was observed that hysteresis can occur and that, in physically symmetrical structures, the symmetrical solution is unstable. It was observed that part of the solution for TE, and TM modes is unstable and followed a route to chaos through period doubling as the guided wave power increased. In general, the stability characteristics of TE and TM waves are similar.

It is worth mentioning that the present solution can be applied to non Kerr-type nonlinearities, as well as to structures with a gradual low power refractive index distribution. It can also be applied to multilayered structures.

As a final remark, the solutions here considered as stable showed excellent agreement with the analytical, stationary solution found in the literature. As not much result is available in the literature concerning the stability characteristics of the higher order modes, no comparison could be made for the solutions here

considered as unstable. Undoubtedly, more investigation is required on this subject, especially experimental investigation, in order to confirm the theoretical and numerical predictions.

ACKNOWLEDGEMENT: This work was supported by TELEBRÁS through the contract PUC-TELEBRÁS 415/91.

REFERENCES

1 - C. T. Seaton, Xu Mai, G. I. Stegeman, e H. G. Winful, *Optical Engineering*, Vol. 24, 1985, pp. 593-599.  
2 - C. K. R. T. Jones e J. V. Moloney, *Phys. Lett. A*, Vol. 117, 1986, pp. 175-180.  
3 - J. V. Moloney, J. Ariyasu, C. T. Seaton, e G. I. Stegeman, *Appl. Phys. Lett.*, Vol. 48, 1986, pp. 826-828.  
4 - J. V. Moloney, J. Ariyasu, C. T. Seaton, e G. I. Stegeman, *Opt. Lett.*, Vol. 11, 1986, pp. 315-317.  
5 - L. Leine, Ch. Wachter, U. Langbein, e F. Lederer, *Opt. Lett.*, Vol. 11, 1986, pp. 590-592.  
6 - L. Leine, Ch. Wachter, U. Langbein, e F. Lederer, *Opt. Lett.*, Vol. 12, 1987, pp. 747-749.

7 - J. Ariyasu, C. T. Seaton, G. I. Stegeman, e J. V. Moloney, *IEEE J. Quantum Electron.*, Vol. QE-22, 1986, pp. 984-987.  
8 - K. Hayata e M. Koshiba, *Opt. Lett.*, Vol. 13, 1988, pp. 1041-1043.  
9 - A. C. P. Zabeu, *MSc Dissertation*, PUC/Rio, 1990 (in Portuguese).  
10 - A. C. P. Zabeu e J. R. Souza, *Proc. 20th European Microwave Conference*, Budapeste, Hungria, 1990, pp. 481-486.  
11 - A. C. P. Zabeu e J. R. Souza, *Microwave and Optical Technology Lett.*, Vol. 3, 1990, pp. 298-302.  
12 - B. M. A. Rahman, J. R. Souza, e J. B. Davies, *IEEE Photonics Technol. Lett.*, Vol. 2, 1990, pp. 265-267.  
13 - C. T. Seaton, J. Valera, R. L. Shoemaker, G. I. Stegeman, J. Chilwell, e S. D. Smith, *IEEE J. Quantum Electron.*, Vol. QE-21, 1985, pp. 774-783.  
14 - K. Ogusu, *IEEE Trans. Microwave Theory and Tech.*, vol. MTT-37, pp 941-946, 1989.